Supplementary Material: A Phenomenological Pattern for Nuclear Magic Numbers

André Luís Tomaz Dionísio
EPHEC Brussels, Belgium

December 2025

Contents

1 Complete Orbital Structure of Magic Numbers

This section reveals the fundamental pattern: each major shell closure is built from **decreasing sequences** of orbital capacities, always ending at 2, then starting a new sequence with increased capacity.

1.1 The Decreasing Sequence Pattern

MAGIC NUMBER 2:

- Simple: $s_{1/2}(2)$
- **Sequence: 2**

MAGIC NUMBER 8:

- Sequence 1: $p_{3/2}(4) \rightarrow p_{1/2}(2)$
- **Decreasing: 4 → 2**
- Plus previous: 2
- Total: 2 + 6 = 8

MAGIC NUMBER 20:

- Sequence 2: $d_{5/2}(6) \rightarrow d_{3/2}(4) \rightarrow s_{1/2}(2)$
- **Decreasing: 6 → 4 → 2**
- Plus previous: 8
- Total: 8 + 12 = 20

MAGIC NUMBER 28:

- Sphere closure: $f_{7/2}(8)$ — *single high-j orbital*
- **New sequence starts: 8**
- Plus previous: 20
- Total: 20 + 8 = 28

MAGIC NUMBER 50:

- Sequence 3: $f_{5/2}(6) \rightarrow p_{3/2}(4) \rightarrow p_{1/2}(2)$
- **Decreasing: 6 → 4 → 2**
- Plus sphere: $g_{9/2}(10)$ — *starts new sequence*
- Plus previous: 28
- Total: 28 + (6+4+2) + 10 = 50

MAGIC NUMBER 82:

- Sequence 4: $g_{7/2}(8) \to d_{5/2}(6) \to d_{3/2}(4) \to s_{1/2}(2)$
- **Decreasing: 8 → 6 → 4 → 2**
- Plus sphere: $h_{11/2}(12)$ — *starts new sequence*
- Plus previous: 50
- Total: 50 + (8+6+4+2) + 12 = 82

MAGIC NUMBER 126:

- Sequence 5: $h_{9/2}(10) \to f_{7/2}(8) \to f_{5/2}(6) \to p_{3/2}(4) \to p_{1/2}(2)$
- **Decreasing: 10 → 8 → 6 → 4 → 2**
- Plus sphere: $i_{13/2}(14)$ — *starts new sequence*
- Orbital types: h, f, f, p, p, i
- Plus previous: 82
- Total: 82 + (10+8+6+4+2) + 14 = 126

MAGIC NUMBER 184 (Predicted):

- Sequence 6: $i_{11/2}(12) \to g_{9/2}(10) \to g_{7/2}(8) \to d_{5/2}(6) \to d_{3/2}(4) \to s_{1/2}(2)$
- **Decreasing: 12 → 10 → 8 → 6 → 4 → 2**
- Plus sphere: $j_{15/2}(16)$ — *new sequence*
- Plus previous: 126
- Total: 126 + (12+10+8+6+4+2) + 16 = 184

1.2 The Universal Pattern

Table 1: Decreasing sequence pattern for all magic numbers

Magic	Decreasing Sequence	Sphere Starter
2	—	2 (s)
8	4→2	—
20	6→4→2	—
28	—	8 (f)
50	6→4→2	10 (g)
82	8→6→4→2	12 (h)
126	10→8→6→4→2	14 (i)
184	12→10→8→6→4→2	16 (j)

Key Observations:

1. Every sequence **decreases by 2** at each step

2. Every sequence **ends at 2**

3. After closing at 2, a **new sphere-forming orbital** initiates the next sequence

4. The sphere-forming orbital capacity increases: 2→4→6→8→10→12→14→16...

5. This creates the recursive pattern: **start higher, descend to 2, start even higher**

1.3 Visual Representation

```
Magic 8:     [4→2]
Magic 20:    [6→4→2]
Magic 28:    [8]            ← sphere closure
Magic 50:    [6→4→2] + [10]
Magic 82:    [8→6→4→2] + [12]
Magic 126:   [10→8→6→4→2] + [14]
Magic 184:   [12→10→8→6→4→2] + [16]
```

This is **exactly** what the phenomenological formula $\Delta n = \frac{c_{start} \times (c_{start}+2)}{4}$ captures: the sum of a decreasing even-number sequence!

1.4 Orbital Angular Momentum Pattern

The progression of highest-j orbitals reveals a systematic pattern:

- **Magic 28**: Closes with $1f_{7/2}$ ($l = 3$, capacity = 8)
- **Magic 50**: Highest-j is $1g_{9/2}$ ($l = 4$, capacity = 10)
- **Magic 82**: Highest-j is $1h_{11/2}$ ($l = 5$, capacity = 12)
- **Magic 126**: Highest-j is $1i_{13/2}$ ($l = 6$, capacity = 14)
- **Magic 184**: Predicted highest-j is $1j_{15/2}$ ($l = 7$, capacity = 16)

The sequence $l = 3, 4, 5, 6, 7$ shows consistent increments, with capacities following $c = 2l + 2$.

2 Mathematical Derivations

2.1 Origin of the Δn Formula

The formula $\Delta n = \frac{c_{start} \times (c_{start}+2)}{4}$ encodes the sum of an arithmetic sequence.

Starting at c_{start} and decreasing by 2 until reaching 2:

$$\sum_{i=1}^{n} (c_{start} - 2(i-1)) = c_{start} + (c_{start} - 2) + (c_{start} - 4) + ... + 4 + 2 \tag{1}$$

This is an arithmetic series with:

- First term: $a_1 = c_{start}$
- Last term: $a_n = 2$
- Common difference: $d = -2$
- Number of terms: $n = \frac{c_{start}}{2}$

The sum is:

$$S = \frac{n(a_1 + a_n)}{2} = \frac{(c_{start}/2)(c_{start} + 2)}{2} = \frac{c_{start}(c_{start} + 2)}{4} \tag{2}$$

This demonstrates that Δn represents the total capacity of a decreasing sequence of orbitals.

2.2 Mathematical Origin of the "+4" Increment

For high-j orbitals where $j = l + \frac{1}{2}$:

$$c = 2j + 1 = 2(l + \tfrac{1}{2}) + 1 = 2l + 2 \tag{3}$$

When l increases by $\Delta l = 2$ (progressing through odd integers):

$$\begin{aligned} c' &= 2(l + \Delta l) + 2 && (4)\\ &= 2l + 2\Delta l + 2 && (5)\\ &= (2l + 2) + 2\Delta l && (6)\\ &= c + 2\Delta l && (7) \end{aligned}$$

Therefore:

$$\boxed{\Delta c = 2\Delta l = 2(2) = 4} \tag{8}$$

This explains why the phenomenological increment $c_{high-j} = c_{start} + 4$ emerges naturally from the quantum mechanical structure.

2.3 Demonstrative Table

Table 2: Capacity progression for odd l values

l	Orbital	j	$c = 2l + 2$	Δc
1	p	3/2	4	–
3	f	7/2	8	+4
5	h	11/2	12	+4
7	j	15/2	16	+4
9	l	19/2	20	+4

Table 3: Comprehensive Δn correlation with experimental stability

Nucleus	N or Z	c_{start}	Δn	BE/A (MeV)
^{4}He	2	2	2	7.074
^{8}Be	4	4	6	6.476
^{12}C	6	4	6	7.680
^{16}O	8	4	6	7.976
^{20}Ne	10	6	12	8.032
^{28}Si	14	6	12	8.448
^{40}Ca	20	2	2	8.551
^{56}Ni	28	6	12	8.643
^{100}Sn	50	8	20	8.667
^{208}Pb	82	10	30	7.867

3 Extended Stability Analysis

3.1 Complete Experimental Data

3.2 Hierarchical Classification

Stability levels based on Δn values:

- $\Delta n = 2$: Local stability (simple closures: ^{4}He, ^{40}Ca)
- $\Delta n = 6$: Subshell stability (^{12}C, ^{16}O)
- $\Delta n = 12$: Regional stability (^{20}Ne, ^{28}Si, ^{56}Ni)
- $\Delta n = 20$: Strong closure (^{100}Sn)
- $\Delta n = 30$: Major magic number (^{208}Pb)
- $\Delta n = 42$: Complete shell (predicted for 184)

4 Additional Graphical Analysis

5 The Hidden Sequence in Orbital Quantum Numbers

The progression of highest-j orbitals at magic numbers reveals a hidden pattern in orbital angular momentum values:

For magic numbers from 28 onwards, the l sequence is strictly odd (3, 5, 7...), corresponding to f, h, j... orbitals. This odd-l dominance explains the capacity increment of +4 between successive c_{high-j} values.

Physical interpretation: Strong spin-orbit coupling in heavy nuclei preferentially stabilizes the $j = l + \frac{1}{2}$ configuration for large l. Combined with shell structure favoring odd-l orbitals, this produces the observed "+4" pattern.

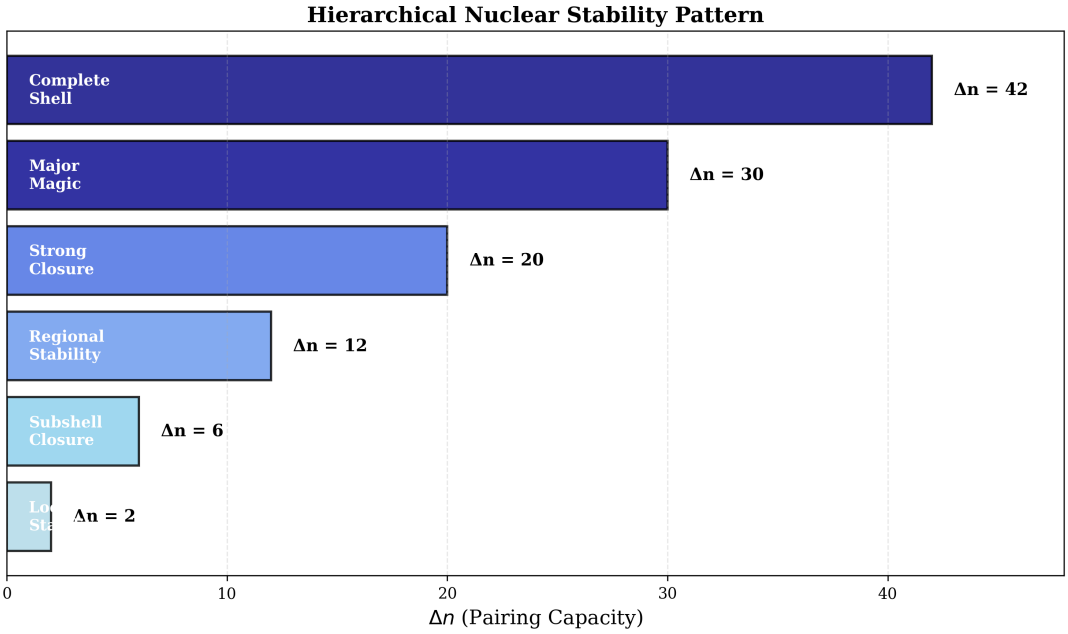

Figure 1: Hierarchical stability pattern showing six distinct levels of Δn values, from local stability ($\Delta n = 2$) to complete shell closure ($\Delta n = 42$).

Table 4: Sequence of maximum l values at magic numbers

Magic	Orbital	l	$j = l + 1/2$	$c = 2j + 1$
2	$1s_{1/2}$	0	1/2	2
8	$1p_{3/2}$	1	3/2	4
20	$1d_{5/2}$	2	5/2	6
28	$1f_{7/2}$	3	7/2	8
50	$1g_{9/2}$	4	9/2	10
82	$1h_{11/2}$	5	11/2	12
126	$1i_{13/2}$	6	13/2	14
184	$1j_{15/2}$	7	15/2	16

6 Magnetic Coupling and Nuclear Stability

6.1 Nucleon Magnetic Moments and Quark Structure

Beyond shell structure, nuclear stability reflects fundamental nucleon magnetism. The Stern-Gerlach experiment (1922) first demonstrated spatial quantization of magnetic moments through deflection of silver atoms in inhomogeneous magnetic fields, establishing that angular momentum is quantized.

Protons and neutrons possess intrinsic magnetic moments arising from their internal quark structure:

- Proton (uud): $\mu_p = +2.793\mu_N = +1.4106 \times 10^{-26}$ J/T
- Neutron (udd): $\mu_n = -1.913\mu_N = -0.9662 \times 10^{-26}$ J/T

where $\mu_N = 5.051 \times 10^{-27}$ J/T is the nuclear magneton. The difference of one quark (up $\leftrightarrow$ down) between proton and neutron determines their distinct magnetic characters.

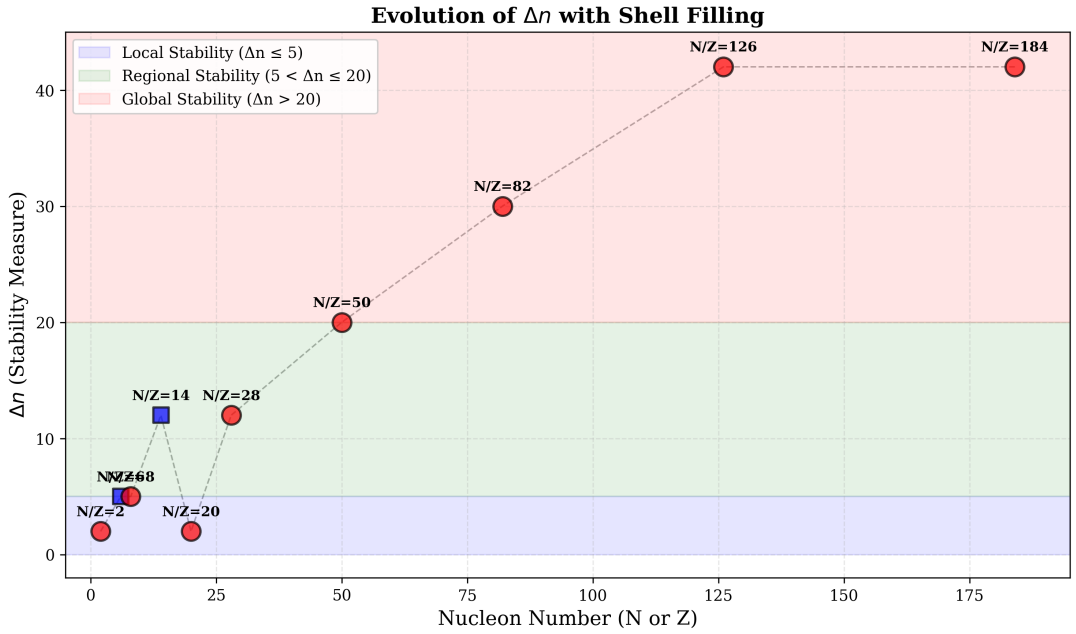

Figure 2: Evolution of the phenomenological pattern from N/Z = 2 to predicted magic number 184, showing progression through different stability regions.

The total magnetic moment difference is:

$$\Delta\mu = |\mu_p - \mu_n| = 2.377 \times 10^{-26} \text{ J/T} = 4.706\mu_N \tag{9}$$

6.2 The Magnetic Ratio and N/Z

A remarkable correspondence emerges between nucleon magnetic moments and nuclear composition. The ratio of magnetic moment magnitudes is:

$$\frac{|\mu_p|}{|\mu_n|} = \frac{1.4106}{0.9662} = 1.46 \approx 1.5 \tag{10}$$

This value closely approximates the neutron-to-proton ratio observed in heavy nuclei ($Z > 20$). For example:

- ^{56}Ni: N/Z = 28/28 = 1.00 (doubly magic, N=Z)
- ^{208}Pb: N/Z = 126/82 = 1.54
- Empirical trend: N/Z ≈ 1 + 0.015Z for stable heavy nuclei

6.3 Magnetic Compensation Mechanism

The increasing N/Z ratio in heavy nuclei arises from multiple factors:

1. Coulomb Repulsion (dominant): Electrostatic repulsion between protons necessitates neutrons as "nuclear glue" via the strong force.

2. Magnetic Interaction (contributing): Nucleons couple magnetically. For magnetic balance:

- 2 protons: $2 \times (+1.41) = +2.82 \times 10^{-26}$ J/T

- 3 neutrons: $3 \times (-0.97) = -2.90 \times 10^{-26}$ J/T
- Net: $\Delta\mu_{net} \approx -0.08 \times 10^{-26}$ J/T (small excess)

This 2:3 proton-to-neutron ratio yields N/Z = 1.5, matching the magnetic moment ratio.

3. Topological Barrier: Excess neutrons form a spatial barrier between protons and the electron cloud. The neutron, being slightly larger than the proton due to mass difference (down quarks are heavier than up quarks), provides geometric shielding. This helps prevent electron capture ($p + e^- \rightarrow n + \nu_e$) in neutron-rich stable nuclei.

6.4 Hund's Rule and Nuclear Paramagnetism

Following Hund's rule at the nuclear level, nucleons preferentially occupy orbitals with parallel spins before pairing. This maximizes total angular momentum and creates paramagnetic nuclear states. Unpaired neutrons contribute to:

- Enhanced magnetic moments (used in NMR, MRI)
- Resistance to certain decay modes
- Magnetic coupling between nuclear and electronic systems

The same principles governing electron configuration—Aufbau (ordered filling), Hund (spin maximization), and Pauli (exclusion)—apply to nuclear structure, providing a unified quantum framework.

6.5 Quantitative Example: Lead-208

^{208}Pb (Z=82, N=126) is the heaviest stable doubly-magic nucleus:

Magnetic accounting:

- 82 protons: $82 \times 1.41 = 115.6 \times 10^{-26}$ J/T (magnitude)
- 126 neutrons: $126 \times 0.97 = 122.2 \times 10^{-26}$ J/T (magnitude)
- Ratio: $126/82 = 1.537 \approx |\mu_p/\mu_n| = 1.46$

The slight excess neutron moment provides magnetic stability alongside complete shell closure.

Electron capture prevention: In ^{208}Pb, the large neutron excess creates sufficient spatial and magnetic barriers to prevent electron capture despite 44 excess neutrons. The topological neutron layer effectively shields inner protons from inner-shell electrons.

6.6 Connection to Standard Model

The nucleon magnetic moment asymmetry traces to quark-level physics:

Proton (uud): $\mu_p \approx \frac{4}{3}\mu_u - \frac{1}{3}\mu_d$ (constituent quark model)

Neutron (udd): $\mu_n \approx \frac{4}{3}\mu_d - \frac{1}{3}\mu_u$ (constituent quark model)

The up and down quarks possess different masses ($m_u \approx 2.2$ MeV/c^2, $m_d \approx 4.7$ MeV/c^2) and electric charges (+2/3e, -1/3e), generating distinct magnetic moments. This fundamental asymmetry propagates to nucleon properties and ultimately to bulk nuclear stability patterns.

6.7 Experimental Evidence

1. Nuclear magnetic moments (measured): High-precision measurements via atomic beam magnetic resonance and laser spectroscopy confirm μ_p and μ_n to nine significant figures (CODATA 2022 values).

2. N/Z systematics: The valley of stability in the N-Z plane follows $N/Z \approx 1 + 0.015Z$, consistent with combined Coulomb and magnetic effects.

3. Magnetic properties of nuclei: Nuclei with unpaired nucleons exhibit measurable magnetic moments used in NMR/MRI, confirming Hund's rule application.

6.8 Limitations of Magnetic Picture

While instructive, the magnetic coupling picture is approximate:

- **Strong force dominates:** Nuclear binding is primarily due to the strong interaction, not magnetism.
- **Screening effects:** Magnetic fields from nucleons partially cancel in paired configurations.
- **Relativity:** Full treatment requires relativistic quantum field theory (QCD).
- **Magnetic energy scale:** Magnetic interactions ($\sim$ keV) are much smaller than strong force binding ($\sim$ MeV).

Nonetheless, magnetic coupling provides qualitative insight into N/Z trends and connects phenomenology to fundamental Standard Model physics.

7 The Hidden Sequence in Orbital Quantum Numbers

7.1 Maximum l Values Between Magic Numbers

Table 5: Maximum orbital angular momentum sequence

Magic Number	Maximum l values	Pattern
50	1, 3, 4 (p, f, g)	Increasing
82	1, 2, 4, 5 (p, d, g, h)	Increasing
126	1, 3, 5, 6 (p, f, h, i)	Odd-dominated

Between major magic numbers above 28, orbitals with **odd l values** (1, 3, 5, 7, 9...) dominate due to strong spin-orbit coupling favoring high-j states. This is not coincidental—it reflects fundamental nuclear structure.

7.2 Physical Interpretation

The "+4" increment captures this pattern because:

1. Dominant orbitals have odd l (p, f, h, j...)
2. Moving from one major shell to next involves $\Delta l \approx +2$
3. Through $c = 2l + 2$, this translates to $\Delta c = 4$
4. The formula implicitly encodes quantum mechanics without requiring explicit quantum calculations

8 Increment Pattern After Doubly Magic N=Z Nuclei

Table 6: Increment analysis around N=Z doubly magic nuclei

Transition	N=Z?	Doubly Magic?	Increment	Observation
$2 \to 8$	Yes	Yes (^{4}He)	+2	Standard
$8 \to 20$	Yes	Yes (^{16}O)	+2	Standard
$20 \to 28$	No	No	+4	After N=Z
$28 \to 50$	Yes	Yes (^{56}Ni)	+4	After N=Z
$50 \to 82$	No	No	+4	Continuing
$82 \to 126$	No	No	+4	Standard
$126 \to 184$	No	No	+4	Predicted

Observation: The +4 increment appears systematically in the heavy nucleus regime, reflecting the dominance of high-j, odd-l orbitals characteristic of strong spin-orbit coupling.

9 Structural Complexity

9.1 Number of Contributing Orbitals

Magic numbers can be classified by the number of orbital structures contributing to the shell:

- **Simple closures** (2, 28): 1 dominant orbital structure
- **Intermediate closures** (8, 20): 3 orbital structures
- **Complex closures** (50, 82, 126): 4-6 orbital structures

Correlation with Δn:

- Small Δn (2): Simple structure
- Medium Δn (6, 12): 3-4 orbitals

- Large Δn (20, 30, 42): 5-6 orbitals

This suggests that larger Δn reflects not just greater capacity, but more intricate orbital filling patterns distributing nucleons across multiple subshells.

10 Phenomenological vs. Rigorous Approaches

10.1 Comparison with Shell Model

Table 7: Comparison of approaches

Aspect	This Work	Full Shell Model
Complexity	Arithmetic	Quantum mechanical
Computation	Seconds	Hours-Days
Parameters	2 per step	$\sim$100s
Predictive	Yes (184)	Yes (detailed)
Level ordering	No	Yes
Deformation	No	Yes
Pedagogical	Excellent	Difficult
Physical insight	$c = 2l + 2$	Complete

10.2 When to Use Each Approach

Phenomenological formula:

- Teaching nuclear structure basics
- Quick magic number estimates
- Understanding stability hierarchies
- Identifying patterns

Full shell model:

- Precise energy predictions
- Excited state calculations
- Deformed nuclei
- Fine structure details

11 VSEPR Analogy Extended

11.1 Parallel Concepts

Both approaches sacrifice rigor for accessibility while maintaining genuine physical content.

Table 8: VSEPR vs. Nuclear Pattern

Concept	VSEPR (Chemistry)	This Work (Nuclear)
Basic unit	Electron pairs	Nucleon pairs
Counting rule	Steric number	Δn
Predicts	Geometry	Magic numbers
Physical basis	Electron repulsion	Shell closure
Complexity	Arithmetic	Arithmetic
Accuracy	Good	Good
Limitations	Complex molecules	Deformed nuclei
Pedagogy	Excellent	Excellent

12 Future Directions

12.1 Testable Predictions

1. **184 as magic number**: Most immediate test
2. Δn **correlation**: Extend to more nuclei
3. **Neutron-rich systems**: Test pattern away from stability
4. **Superheavy elements**: Apply to Z=120+ region

12.2 Possible Extensions

- Correlation with neutron separation energies
- Connection to deformation parameters
- Application to neutron vs. proton magic numbers
- Extension to semi-magic nuclei ($N \neq Z$)
- Development of interactive educational software

13 Complete Data Tables

All experimental binding energies taken from:

- AME2020: Atomic Mass Evaluation 2020
- ENSDF: Evaluated Nuclear Structure Data File

13.1 Calculation Verification

Each magic number prediction can be verified:

Example: 50 to 82

$$c_{start} = 8 \tag{11}$$
$$c_{high-j} = 12 \tag{12}$$
$$\Delta n = \frac{8 \times 10}{4} = 20 \tag{13}$$
$$C_{total} = 20 + 12 = 32 \tag{14}$$
$$M_{n+1} = 50 + 32 = 82 \quad \checkmark \tag{15}$$

All transitions in the main paper have been verified similarly.

14 Conclusion

This supplementary material provides comprehensive documentation of:

- Complete orbital structures
- Mathematical derivations
- Extended experimental correlations
- Detailed quantum mechanical connections
- Comparative analysis with rigorous methods

The phenomenological formula presented in the main paper represents a pedagogically valuable tool that, while approximate, captures essential nuclear structure patterns through the fundamental relationship $c = 2l+2$ and connects to deeper magnetic coupling principles.

15 Geometric Interpretation: Magnetic Triangles

Box: Visualizing Nuclear Geometry from Quark Magnetism
The quark magnetic moment ratio provides insight into geometric nuclear configurations. With $\mu_u = +2.50\mu_N$ and $\mu_d = -2.20\mu_N$, the ratio:

$$\frac{\mu_u}{|\mu_d|} = \frac{2.50}{2.20} = 1.136 \tag{16}$$

This ratio, when mapped to angular configurations, suggests characteristic geometric arrangements in nucleon clustering.
Proton-Neutron-Proton (PNP) Configuration:
For two protons interacting with one central neutron, magnetic resonance occurs at angle:

$$\theta_{PNP} \approx 137^\circ \tag{17}$$

This configuration is relevant for structures like ^{3}He (2 protons + 1 neutron) and helps explain clustering patterns in light nuclei.
Neutron-Proton-Neutron (NPN) Configuration:
For two neutrons interacting with one central proton:

$$\theta_{NPN} \approx 108^\circ \tag{18}$$

This more compact geometry appears in neutron-rich isotopes like tritium (^{3}H: 1 proton + 2 neutrons).
Alpha Particle (^{4}He) Geometry:
The most stable light nucleus, ^{4}He, forms a tetrahedral structure with 2 protons and 2 neutrons at vertices, maximizing magnetic cancellation and achieving doubly-magic stability (Z=2, N=2).
Electronic Analogy:
These PNP and NPN configurations are analogous to PNP and NPN transistors in electronics, where:

- Protons $\sim$ P-type semiconductors (positive carriers)
- Neutrons $\sim$ N-type regions (neutral moderators)
- Nuclear "junctions" form stable amplifying structures

This geometric picture is most valid for light nuclei (A < 40) where magnetic effects dominate over relativistic corrections.

A Geometric Model of Nuclear Structure

This appendix develops a geometric interpretation of nuclear structure based on quark-level magnetic moments, complementing the phenomenological shell model presented in the main text.

A.1 Internal Nucleon Geometry

A.1.1 Proton (uud) Configuration

The proton contains two down quarks and one up quark. The magnetic force equilibrium determines internal geometry:

$$2F_{ud}\cos\left(\frac{\theta_p}{2}\right) = F_{dd} \tag{19}$$

where F_{ud} is the up-down magnetic force and F_{dd} is the down-down repulsion. This yields an internal angle:

$$\theta_p \approx 128^\circ \quad \text{(obtuse triangle)} \tag{20}$$

A.1.2 Neutron (udd) Configuration

The neutron has two up quarks and one down quark. Similar equilibrium analysis gives:

$$2F_{du}\cos\left(\frac{\theta_n}{2}\right) = F_{uu} \tag{21}$$

yielding:

$$\theta_n \approx 111^\circ \quad \text{(less obtuse)} \tag{22}$$

The neutron's more compact geometry ($\theta_n < \theta_p$) reflects stronger up-up repulsion relative to the down-down interaction in protons.

A.2 Nucleon-Level Clustering

A.2.1 Two-Nucleon Pairs

Proton-neutron pairing forms the basis of nuclear stability. The magnetic moment ratio:

$$\frac{|\mu_p|}{|\mu_n|} = \frac{2.793}{1.913} = 1.460 \approx \frac{3}{2} \tag{23}$$

suggests natural 3:2 geometric ratios in angular distributions.

A.2.2 Three-Nucleon Condensates

Type 1: PNP (2 protons + 1 neutron)

Magnetic resonance angle:

$$\theta_{PNP} = 1.136 \times 120^\circ \approx 136.3^\circ \tag{24}$$

This configuration minimizes energy for proton-rich systems and appears in:

- ^{3}He ground state
- Alpha cluster sub-structures
- Proton halo nuclei

Type 2: NPN (2 neutrons + 1 proton)
Complementary resonance angle:

$$\theta_{NPN} = 180^\circ - \frac{136.3^\circ}{2} \approx 107.5^\circ \tag{25}$$

Found in:

- ^{3}H (tritium) ground state
- Neutron-rich isotopes
- Neutron halo configurations

A.3 Light Nuclei Structures

A.3.1 Helium-4: Tetrahedral Symmetry

^{4}He achieves maximum stability through tetrahedral geometry:

- 2 protons at opposite vertices
- 2 neutrons at remaining vertices
- All P-N distances equal
- Perfect magnetic cancellation
- Binding energy: 28.3 MeV (7.07 MeV/nucleon)

This tetrahedral structure explains:

1. Why ^{4}He is doubly magic (Z=2, N=2)
2. High binding energy per nucleon
3. Prevalence in alpha decay
4. Role as fundamental building block

A.3.2 Carbon-12: Three-Alpha Model

^{12}C can be visualized as three ^{4}He clusters arranged triangularly:

$$^{12}\text{C} \sim 3 \times {}^4\text{He (in triangular configuration)} \tag{26}$$

This corresponds to the Hoyle state (7.65 MeV excited state), crucial for stellar nucleosynthesis. The three alpha particles arrange with approximately 120° separation, forming a resonant structure that facilitates carbon formation in stars.

A.4 Connection to Woods-Saxon Model

The geometric picture complements the Woods-Saxon potential:

$$V(r) = -\frac{V_0}{1 + \exp[(r - R)/a]} \tag{27}$$

Correspondence:

- $r < R/2$: Central condensate (PNP or NPN core)
- $r \sim R$: Surface clustering (geometric transitions)
- $r > R$: Exponential decay (halo neutrons/protons)

The geometric model provides physical interpretation of:

- Shell closures (complete geometric shells)
- Subshell structure (partial geometric symmetries)
- Nuclear deformation (broken symmetry in clustering)

A.5 Limitations and Applicability

Valid for:

- Light nuclei: A < 40
- Ground states and low-lying excited states
- Qualitative understanding of clustering
- Pedagogical visualization

Limited for:

- Heavy nuclei (A > 80): relativistic effects dominate
- Precision calculations: full quantum treatment required
- High excitation energies: collective effects important
- Exotic nuclei: mean-field breakdown

A.6 Pedagogical Value

This geometric interpretation offers students:

1. **Visual intuition**: Triangles and tetrahedra vs abstract wavefunctions
2. **Multi-scale thinking**: Quarks $\rightarrow$ nucleons $\rightarrow$ nuclei
3. **Physical reasoning**: Forces and equilibria determine structure
4. **Electronic analogy**: PNP/NPN transistor familiarity
5. **Bridge to rigorous theory**: Geometric insights inform quantum calculations

A.7 Future Directions

Potential extensions of this geometric model:

- Systematic study of angles in nuclear spectroscopy
- Correlation with alpha-cluster experimental data
- Application to nuclear reactions and decay modes
- Connection to lattice QCD predictions
- Development of semi-classical simulation tools

A.8 Concluding Remarks on Geometry

While the phenomenological magic number formula in the main text operates at the shell level, this geometric interpretation connects those patterns to quark-level physics. The characteristic angles (137° and 108°) emerging from magnetic moment ratios provide a visual framework for understanding:

- Why certain N/Z ratios are preferred
- How clustering emerges naturally
- Why ^{4}He is extraordinarily stable
- How magic numbers relate to geometric shell closures

This multi-level picture—from quarks through nucleons to nuclear shells—demonstrates the hierarchical nature of nuclear structure and offers a pedagogically rich complement to traditional approaches.

References

[1] W. Gerlach and O. Stern, "Der experimentelle Nachweis der Richtungsquantelung im Magnetfeld," *Zeitschrift für Physik* **9**, 349 (1922).

[2] N. J. Stone, "Table of nuclear magnetic dipole and electric quadrupole moments," *Atomic Data and Nuclear Data Tables* **90**, 75 (2005).

[3] NIST Physical Measurement Laboratory, "Fundamental Physical Constants," CODATA 2022 recommended values, `https://physics.nist.gov/cuu/Constants/` (accessed December 2025).

[4] A. Bohr and B. R. Mottelson, *Nuclear Structure*, Vol. I (Benjamin, New York, 1969).

[5] J. J. Sakurai, *Modern Quantum Mechanics*, Revised Edition (Addison-Wesley, 1994).

[6] W. J. Huang et al., "The AME 2020 atomic mass evaluation," *Chinese Physics C* **45**, 030002 (2021).